Apr 1st, 8:00 AM

The Theoretical Signal Strength Reduction on the Air Force Eastern Test Range

Charles C. Sellers
RCA International Service Corporation, Missile Test Project

Scholarly Commons Citation

Sellers, Charles C., "The Theoretical Signal Strength Reduction on the Air Force Eastern Test Range" (1971). *The Space Congress® Proceedings*. 1.
https://commons.erau.edu/space-congress-proceedings/proceedings-1971-8th/session-10/1

THE THEORETICAL SIGNAL STRENGTH REDUCTION ON THE AIR FORCE EASTERN TEST RANGE

Charles C. Sellers
RCA International Service Corporation
Missile Test Project
Patrick Air Force Base, Florida

ABSTRACT

Since both metric and non-metric data are transmitted through a missile's antenna system, assurance of an adequate signal level at the ground sites is essential in planning the range instrumentation support of a launch. For this reason a theoretical signal strength reduction is performed at the Air Force Eastern Test Range before every missile launch.

The missile contractor defines the radiation characteristics of each missile-antenna combination in the form of an antenna pattern. The antenna pattern format and the vehicle-antenna coordinate system have been defined by the Inter Range Instrumentation Group. The aspect angles for each tracking site are computed for the theoretical trajectory. These aspect angles are then coupled with the antenna pattern, so that with knowledge of the other parameters, (1) transmitted power; (2) frequency; (3) ground antenna gain, and (4) the polarizations of both antennas, the power received by a ground station can be readily calculated.

INTRODUCTION

RCA's mission of technical support on the Air Force Eastern Test Range includes acquiring data from the flight of each missile and supplying the data to the Range User. These data consist of metric data, such as C-Band Radar data, that specify the location of the missile within a coordinate reference system; and non-metric data, such as the engineering information concerning operation of the missile, that are transmitted through various telemetry links.

Before each launch the range capabilities to obtain these data must be evaluated, and the test support operations must be planned. Of primary importance in the planning is the pre-flight data package generated by RCA Data Reduction. This pre-flight data package is based upon the theoretical, planned trajectory furnished by the missile contractor. These pre-flight data aid in determining which instrumentations will be manned during the test, where the Range Instrumentation Ships will be located, where aircraft data acquisition runs will be made, and what level of data commitments can be met. For example, look angles indicate if and when the range tracking instruments will see the missile. GDOP*computations indicate the expected accuracy of the metric data for various combinations of tracking sites. In addition, it is necessary to evaluate the signal strength that will be obtained at the tracking sites, since both metric and non-metric data are transmitted through the missile's antenna systems. For this reason a theoretical signal strength reduction is performed before each launch. The end product is the expected received signal strength for each of the ground stations and the proposed ship and aircraft test support positions, throughout their respective tracking periods.

The signal strength reduction is an analysis of those factors which determine the received signal level (Figure 1) by use of the specific parameters for a given launch in conjunction with a particular trajectory and a set of antenna patterns. Flame attenuation is not modelled in the reduction, but its presence is implied by the aspect angles included in the final signal strength report as tabulated by the ACES computer program (Figure 10). When the aspect angles show the receiving site to be aligned with the negative roll axis of the missile, (that is, directly behind the missile) flame effects could be considerable. Distance, frequency, polarization, transmitter power, and receiver gain are treated numerically in the ACES program computations. Each combination of a particular antenna with a different missile body has its own characteristic radiation pattern. Each different trajectory presents the tracking site with different aspect angles. The pairing of the antenna pattern with the range and aspect angles is the heart of the signal strength reduction.

THE ANTENNA PATTERN

An antenna pattern is a representation of an antenna's radiation or receiving characteristics in geometric space. These characteristics are usually expressed as contours of equal gain or in numerical matrix form relative to a reference gain. The numerical matrix form of an antenna pattern is developed from a coordinate system defined by the Inter-Range Instrumentation Group (IRIG) in IRIG Document 111-65.

According to the IRIG System, the spherical coordinates defined by IEEE Standards, and already in use for antenna pattern measurements have been perpetuated. In this system the antenna is placed at the center of a theoretical sphere. The sphere

---

* Geometric Dilution of Precision

is encircled by a reference system of phi and theta lines which can be used to specify any point on the sphere, as latitude and longitude are used on the earth. Phi lines are analogous to the meridians of longitude, while theta lines correspond to parallels of latitude. Phi is measured in degrees around the sphere with a range from 0° to 360°. Theta is measured in degrees from 0° to 180°. By specifying the phi-theta coordinates, one may designate points on the imaginary sphere for measurement of the antenna characteristics.

IRIG's addition to the existing system was a standardized orientation for an antenna-bearing vehicle within the coordinate system, as illustrated in Figure 2. The missile, or other antenna-bearing vehicle, is oriented so that its roll axis coincides with the axis of the sphere which extends from the point theta equals 180° to the point theta equals 0°. The point where the negative yaw axis pierces the sphere is designated 0° phi. This point is usually aligned with the dorsal side of the missile. If the missile is viewed from the rear, phi increases clockwise from 0° to 360°. This reference system remains fixed to the missile throughout its flight, regardless of various maneuvers which may re-orient the missile.

The standard coordinate system is used by the missile contractor in generating antenna patterns. He usually fabricates a scale model of the missile with its antennas and measures the signal strength in all directions, over the entire surface of the sphere. The measurements are generally made at 2° increments of phi and theta to produce a complete pattern of 16,380 gain values. The gain is measured in decibels referred to an isotropic antenna.

To display the pattern of gain values, a rectangular matrix of the numerical values is useful. Figure 3 illustrates the relationship between the standard coordinate system and numerical matrix. The cube in the center represents the missile bearing the antenna. The missile's positive roll axis is labelled P_R, the negative pitch axis is P'_p, and the negative yaw axis is P'_y. The gain values recorded on the surface of the sphere are projected outward onto a tangent cylinder, aligned as shown. The cylinder is then split along the phi = 0° meridian and flattened. A partial example is shown in Figure 4. In this example the odd number values have been omitted to emphasize the contours.

This is only a partial representation of an antenna pattern, because it does not include the full range of phi and theta; 0° to 360°, and 0° to 180° respectively. It is also incomplete in that it describes only one of the polarization components. To represent the power transfer between two antennas, the general solution requires consideration of several polarization components. Both the RF wave's intensity and its polarization relative to the receiver are required.

POLARIZATION

The RF wave may be portrayed by the behavior of its electric vector. In the general case the electric vector varies in amplitude at the radio frequency rate in such a way that it may be represented by an ellipse. This is termed elliptical polarization. Linear polarization and circular polarization are the limiting conditions of the more general elliptical polarization. Linear and circular polarization are represented in Figure 5.

A linearly polarized wave is one whose electric vector oscillates along a fixed line at all times. Its magnitude variations are confined to a single plane along a radial line from the source. If the radiated wave is a sinusoidal function, the electric vector at Z=0 changes from positive to negative in a sinusoidal manner.

A linearly polarized receiving antenna with its polarization vector in the same plane and parallel to the electric vector of the incoming wave will receive maximum energy. Any non-alignment of the receiver's polarization vector results in a proportional loss of received power. In this linear-to-linear case the power loss is a function of the square of the cosine of the cross polarization angle beta between the two polarization vectors.

A circularly polarized wave is one whose electric vector is constant in magnitude and which appears to rotate at a constant angular velocity as the wave passes a fixed point. Its angular position is a function of time. A circularly polarized receiver obtains the maximum signal from a circular wave if it is of the same sense --- that is, if both are right-hand circular or if both are left-hand circular. If the sense is opposite, no energy is received. If the transmitter-to-receiver link mismatches linear with circular polarizations (or vice-versa) only half the energy is extracted from the wave; that is, a 3 db loss occurs.

An elliptically polarized wave is one whose electric vectors change in magnitude so as to generate an ellipse, as the wave passes a fixed point. The amount of the available signal which is received depends upon the relative polarization between the wave and the receiving antenna. The ellipse may be resolved into two circular components of opposite sense, as illustrated in Figure 6. Note that the vectors are different in magnitude, and they rotate in opposite directions, but at the same rate. When the vectors coincide the resultant is their sum; when they are opposite, the resultant is their difference. The locus of the resultant is the ellipse. If the two circular component vectors were equal, the resultant would always lie along a straight line, the major axis of the ellipse and result in linear polarization, one limit of elliptical polarization. If, however, one circular component were absent entirely, the one remaining circular component would constitute circular polarization, which is the other limiting case of elliptical polarization.

To fully define the elliptical pattern, six components are recorded. Amplitude measurements g_{ϕ}, g_{45}, g_{θ}, and g_{135}, are recorded along the axes E_{ϕ}, E_{45}, E_{θ}, and E_{135}, as illustrated in Figure 7. Right and left circular components are also recorded. The tilt angle, Tau, is difficult to obtain from direct measurement. However, it may be calculated from the four linear components g_{ϕ}, g_{45}, g_{θ}, and g_{135}, from the following relationships:

$$\tau = \frac{1}{2} \arctan \frac{E^2_{45^\circ} - E^2_{135^\circ}}{E^2_{\theta} - E^2_{\phi}} \qquad (1)$$

or

$$\tau = \frac{1}{2} \arctan \frac{\left[\log^{-1} \frac{g_{45^\circ}}{20}\right]^2 - \left[\log^{-1} \frac{g_{135^\circ}}{20}\right]^2}{\left[\log^{-1} \frac{g_{\theta}}{20}\right]^2 - \left[\log^{-1} \frac{g_{\phi}}{20}\right]^2} \qquad (2)$$

THE ASPECT ANGLES

Figure 8 illustrates the use of the antenna pattern sphere with the aspect angles for the receiving site. Aspect angle theta is measured from the positive roll axis back to the slant range vector. Phi is measured clockwise (as viewed from the rear of the missile) from the dorsal fin to the projection of the slant range vector into the roll plane.

As the missile moves through its trajectory, its attitude relative to the viewing site constantly changes. At each time point in the trajectory, the slant range vector pierces the antenna pattern sphere at a different point. For each different phi-theta point, the ACES computer program selects the gain from the antenna pattern input, for use in computing the signal strength.

Figure 8 implies that the ground antenna is tracking; such is usually the case. Since the range vector intersects the ground antenna pattern at a constant point, it may be defined with a constant gain value. If the ground antenna were fixed, it would be necessary to define the ground gain through use of a ground antenna pattern, in the same way the missile-borne pattern is used. The ground gain for a fixed antenna would be extracted from the series of phi-theta points where the slant range vector pierces the ground antenna pattern sphere, as the missile moves past. In the ground antenna sphere, phi is an azimuth-like measurement, beginning with phi = 0° toward the south, and increasing counterclockwise to 360°. Theta for the ground sphere is measured from vertical downward.

COMPUTATIONS

The basic signal strength equation used in the ACES program is the following:

$$dbm_r = 10 \log_{10} \frac{10^{\left(\frac{dbm_t}{10}\right)} \cdot C^2}{\qquad} (G_{RG}G_{RM} + G_{LG}G_{LM} + 2\,(G_{RG}G_{RM}G_{LG}G_{LM})^{\frac{1}{2}} \operatorname{Cos} 2\beta) \qquad (3)$$

In this equation dbm_r is the expected received power level in decibels referenced to 1 milliwatt; dbm_t is the transmitted power level; the propagation speed, C, is in feet/sec; R is the range in feet; and f is the frequency in HZ. G_{RG} and G_{LG} are the right and left handed ground antenna gain components; and G_{RM}, G_{LM} are the right and left handed missile antenna gain components. Note that these G quantities are actually exponential functions. In each case the subscripted G = $10^{(G'/10)}$ where G' is the gain value in db from the antenna pattern, and the subscripted G is dimensionless. β is the smaller angle between the major axes of the transmitting and receiving ellipses.

P, the polarization mismatch loss which is effected by equation (3), is computed as follows:

$$P = 10 \log \frac{G_{RG}G_{RM}+G_{LG}G_{LM}+2(G_{RG}G_{RM}G_{LG}G_{LM})^{\frac{1}{2}} \cos 2\beta}{(G_{RG} + G_{LG})\ (G_{RM} + G_{LM})} \qquad (4)$$

In computing P, the smaller angle between the major axes of the transmitting and receiving ellipses (β) is calculated as follows:

$$\beta' = \left| \ \tau_m (\phi_m, \theta_m) - (\tau_g (\phi_g, \theta_g) + \overline{\gamma}) \right|_{\text{MODULO } 180^\circ}$$

$$\beta = 180^\circ - \beta' \quad \text{if } \beta' > 90^\circ$$

$$\beta = \beta' \qquad\qquad \text{if } \beta' \leq 90^\circ$$

τ_m and τ_g have already been computed according to equation (2).

The ACES computations are made at regular intervals throughout the trajectory while the viewing sites elevation angles are positive. Each computation of dbm_r requires about 4 seconds of computer time on the IBM 7094 as presently programmed. About half the computer time is spent in searching the magnetic tape input containing the antenna pattern for the applicable phi-theta point. If a large block of disk or drum storage were available to contain the whole antenna pattern at once, ready for direct accessing, the computer time would be reduced considerably.

Figure 9 illustrates the steps which may be involved in the reduction. The computer runs listed on the left are the trajectory generations and manipulations. More or fewer trajectory runs may be required, but they always culminate in the computation of the aspect angles. The antenna pattern data come to the reduction unit in a standardized format prescribed by document AFSCM 80-4, on paper tape or magnetic tape. After tau is computed, the antenna pattern data and the aspect angles enter the ACES computations.

RESULTS

Figure 10 is an example of the ACES theoretical signal strength tabular results. After time, azimuth, elevation, range, and altitude, there is printed the most important column, dbm_r, the expected received signal level. Then there follow the aspect angles, phi and theta; beta, the angle between the antenna reference axes; P, the polarization mismatch loss; GM, the directional gain at the missile; and 20 log range in feet. This particular ACES run was made in support of an ETR Test 4209, the launch of a Minuteman III on 14 December 1970.

Figure 11 is an example of the actual test results from this test. The instrumentations are rate stations of the Mistram continuous wave tracking system. The solid line represents the actual signal level received, while the dashed line is the dbm_r predicted by the ACES program. At the beginning of the tracking period there is an erratic jumping due to low elevation effects not modelled in the theoretical signal strength equation. The elevation angles there are generally below 5 degrees, and track is not expected.

Since the Mistram hardware's accuracy in recording the signal level is about ± 5 db, and other factors may cause deviation from nominal, the correlation between predicted and actual signal is considered excellent. Such results are typical. The value of predicting peaks and nulls such as these is evident.

The signal strength reduction has been successfully applied to the various electronic systems which have been used on the Range. C-band Radar, Glotrac, Udop, Mistram, Command Destruct, and Telemetry systems have all been successfully analyzed.

A RECENT APPLICATION

A recent application of the reduction has been its use for P-band and Unified S-band links used by the Apollo Range Instrumentation Aircraft (ARIA). Each of the eight ARIA contains an airborne telemetry station which supplements land and ship stations in support of Apollo and DOD space and missile programs. Each aircraft is equipped with a 7 foot parabolic antenna with P-band and S-band feeds, telemetry tracking and data receivers, and data storage devices. The ARIA were designed to operate at 30,000 ft. altitude over open ocean. They provide orbital, trans-lunar injection period and re-entry data links with the Apollo spacecraft. A problem in mission support has been the multipath phenomenon which occurs at low telemetry antenna elevation angles. The P-band and S-band antennas receive a reflected signal from the ocean in addition to the direct signal. The reflected signal is considerably delayed in time due to the height of the aircraft and the vehicle, so that destructive interference results. The problem is lessened by an upward beam-tilt of the antenna, so that the reflected signal is partially rejected. However, the destructive interference has made prediction of the received signal difficult. A new signal strength computer program is now being developed to analyze the amount of interference quantitatively. The new program will compute the reflection point on the sea (or land) below, the grazing angle of the reflected ray, phase differences, and net signal strength, among other parameters. It will also include effects of refraction, and losses at the reflection point due to absorption and divergence. The input data will consist of missile and aircraft antenna patterns, a trajectory, and an aircraft flight plan.

Through such new programs, and through the older, established techniques, the signal strength reduction will continue to meet the changing needs of the Range for planning data.

REFERENCES

G. D. Trimble, RCA Computer Program No. 296 (ACES), RCA Computer Program No. 140 (GASP), and RCA Computer Program No. 698 (APPP).

"Power Transfer Between Arbitrarily Polarized Antennas", TM-1071-23, 9 March 1971, by Eugene M. Fetner, RCA International Service Corporation, Missile Test Project, Patrick AFB, Florida.

"IRIG Standard Coordinate System and Data Formats for Antenna Patterns", IRIG Document 111-65, May, 1966, Secretariat, Range Commanders Conference, Attn: STEWS-ROD-RCCC, White Sands Missile Range, New Mexico.

"Missile Antenna Data Requirements", AFSC Manual 80-4, 1 August, 1970, AFSC, Andrews AFB, Washington, D. C.

"Mistram/MRS, Minuteman III Test 4209, System Operation and Data Acquisition", 6 January 1971, RCA International Service Corporation, Missile Test Project, Patrick AFB, Florida.

MAJOR FACTORS WHICH DETERMINE RECEIVED SIGNAL STRENGTH

1. TRANSMITTER POWER
2. RECEIVER GAIN
3. DISTANCE
4. FREQUENCY
5. POLARIZATION MISMATCH
6. ASPECT ANGLE FOR RECEIVING SITE RELATED TO A PARTICULAR ANTENNA-MISSILE COMBINATION
7. FLAME ATTENUATION

FIGURE 1

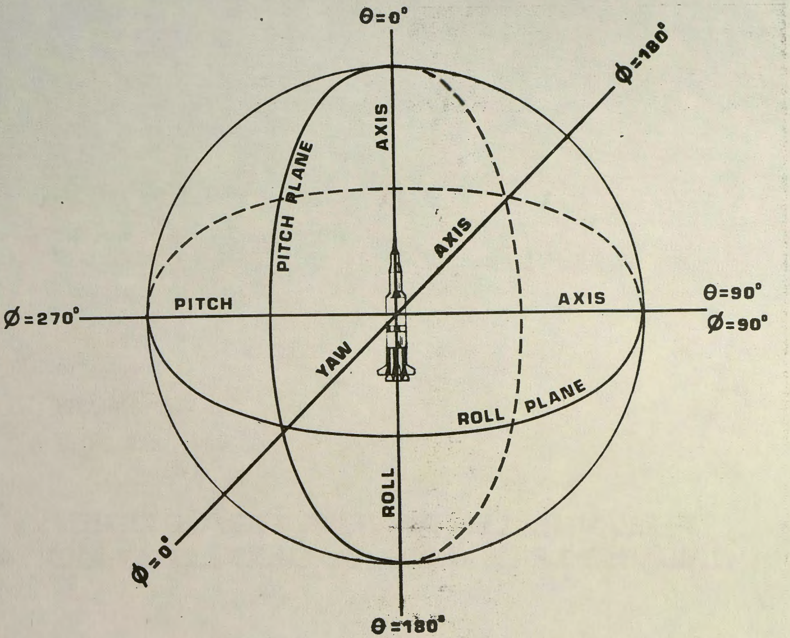
θ=0°
φ=180°
AXIS
PITCH PLANE
AXIS
PITCH
AXIS
θ=90°
φ=90°
φ=270°
YAW
ROLL PLANE
ROLL
φ=0°
θ=180°

FIGURE 2

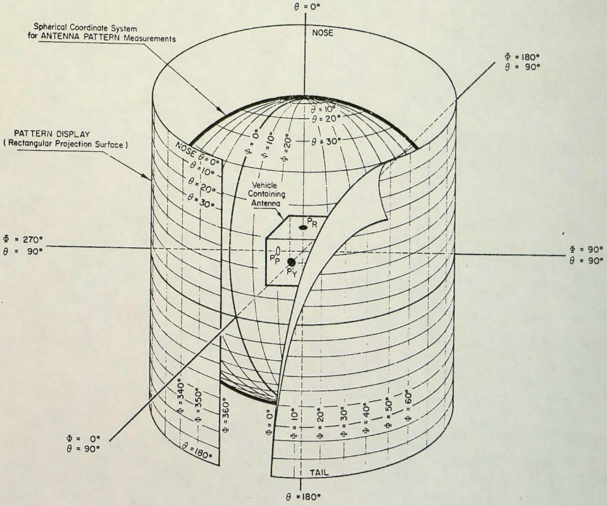
θ = 0°
NOSE
Spherical Coordinate System for ANTENNA PATTERN Measurements
Φ = 180°
θ = 90°
θ = 10°
θ = 20°
θ = 30°
Φ = 0°
Φ = 10°
Φ = 20°
PATTERN DISPLAY (Rectangular Projection Surface)
NOSE θ = 0°
θ = 10°
θ = 20°
θ = 30°
Vehicle Containing Antenna
P_R
0
P_P
P_Y
Φ = 270°
θ = 90°
Φ = 90°
θ = 90°
Φ = 340°
Φ = 350°
Φ = 360°
θ = 180°
Φ = 0°
Φ = 10°
Φ = 20°
Φ = 30°
Φ = 40°
Φ = 50°
Φ = 60°
Φ = 0°
θ = 90°
TAIL
θ = 180°

Figure 3.

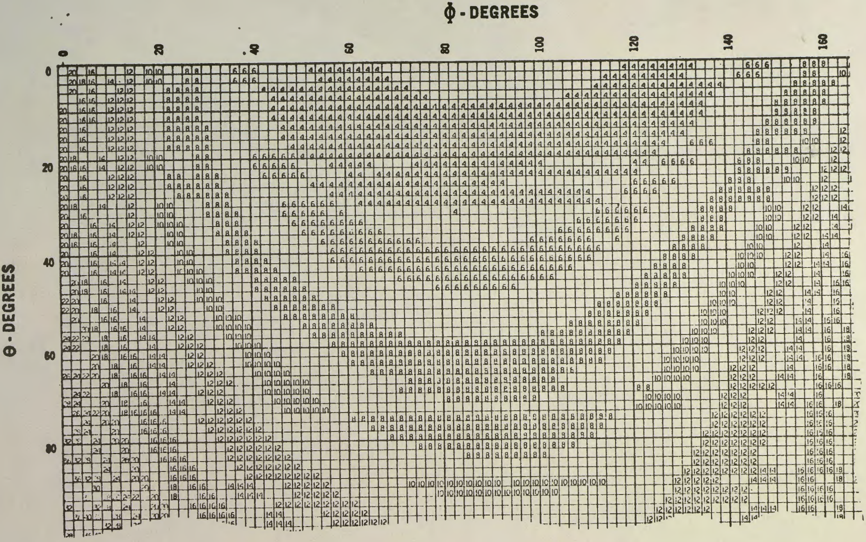

Figure 4 Sample of Matrix Antenna Pattern Plot

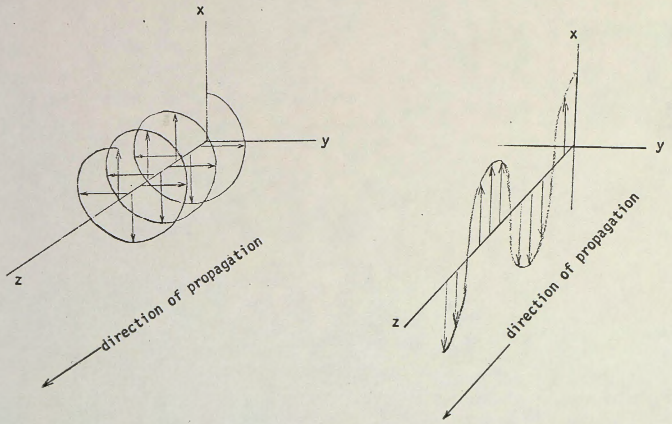

CIRCULARLY POLARIZED WAVE

LINEARLY POLARIZED WAVE

FIGURE 5

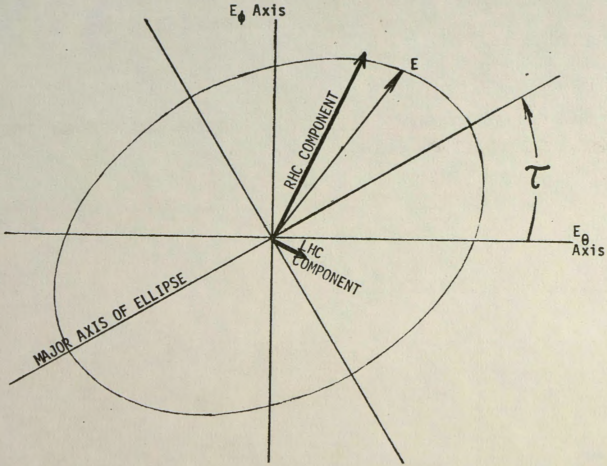
E_ϕ Axis
E
RHC COMPONENT
τ
E_θ Axis
LHC COMPONENT
MAJOR AXIS OF ELLIPSE

FIGURE 6

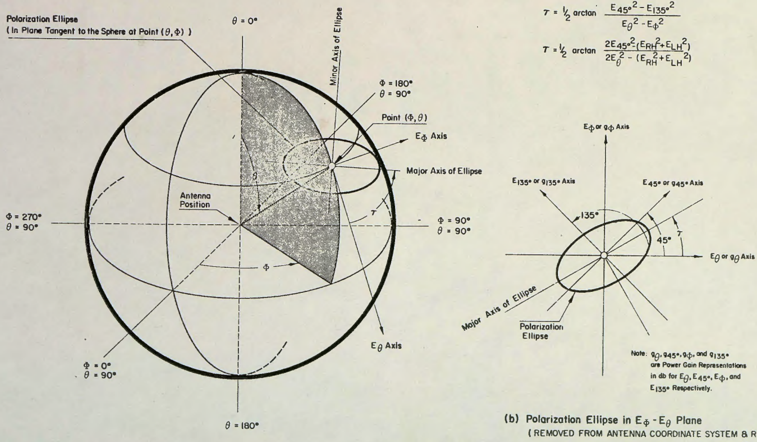

$$\tau = \tfrac{1}{2} \arctan \frac{E_{45°}{}^2 - E_{135°}{}^2}{E_\theta{}^2 - E_\Phi{}^2}$$

$$\tau = \tfrac{1}{2} \arctan \frac{2E_{45°}{}^2 - (E_{RH}{}^2 + E_{LH}{}^2)}{2E_\theta{}^2 - (E_{RH}{}^2 + E_{LH}{}^2)}$$

Note: g_θ, $g_{45°}$, g_Φ, and $g_{135°}$ are Power Gain Representations in db for E_θ, $E_{45°}$, E_Φ, and $E_{135°}$ Respectively.

(b) Polarization Ellipse in $E_\Phi - E_\theta$ Plane
(REMOVED FROM ANTENNA COORDINATE SYSTEM & REORIENTED)

(a) Polarization Ellipse in Reference to Antenna Coordinate System

POLARIZATION ELLIPSE AND POLARIZATION COMPONENTS
FIGURE 7

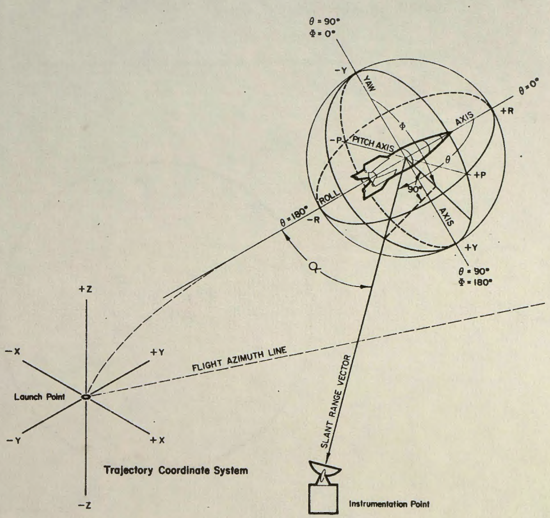
θ = 90°
Φ = 0°
-Y
YAW
θ = 0°
+R
AXIS
Φ
-P
PITCH AXIS
θ
+P
90°
ROLL
AXIS
θ = 180°
-R
+Y
θ = 90°
Φ = 180°
α
+Z
-X
+Y
FLIGHT AZIMUTH LINE
SLANT RANGE VECTOR
Launch Point
-Y
+X
Trajectory Coordinate System
-Z
Instrumentation Point

Figure 8

SIGNAL STRENGTH REDUCTION

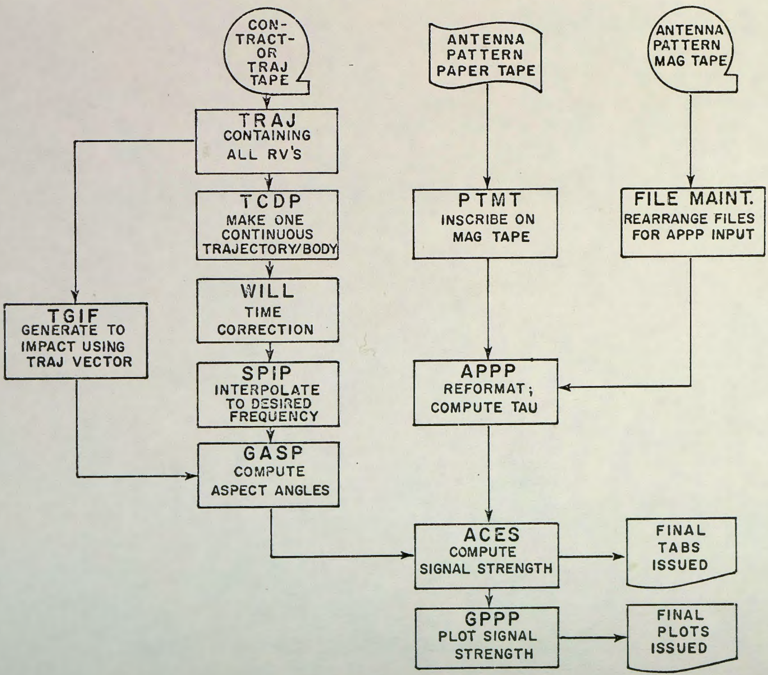

FIGURE 9

NOMINAL LOOK ANGLE, ASPECT ANGLE AND SIGNAL STRENGTH DATA FOR MRS 31

TIME (SEC)	AZIMUTH (DEG.)	ELEVATION (DEG.)	RANGE (K FEET)	ALTITUDE (K FEET)	RCVD PWR LVL (DBM)	PHI (DEG)	THETA (DEG)	BETA (DEG)	P (DB	GM (DB)	20 LOG R
211.00	62.85	35.46	1917.5	1167.7	-96.3	146.7	58.7	0.2	0.	1.8	125.7
212.00	63.16	35.47	1931.5	1177.0	-96.8	147.3	58.7	0.2	0.	1.4	125.7
213.00	63.47	35.48	1945.6	1186.2	-97.0	147.7	58.8	0.2	0.	1.2	125.8
214.00	63.77	35.49	1959.6	1195.5	-96.9	148.2	59.0	0.2	0.	1.4	125.8
215.00	64.07	35.50	1973.7	1204.7	-97.0	148.7	59.3	0.2	0.	1.3	125.9
216.00	64.36	35.51	1987.8	1213.9	-97.1	149.1	59.5	0.2	0.	1.3	126.0
217.00	64.65	35.52	2002.0	1223.1	-97.8	146.0	54.3	0.2	0.	0.7	126.0
218.00	64.93	35.52	2016.1	1232.3	-99.5	140.1	42.8	0.1	0.	-1.0	126.1
219.00	65.22	35.53	2030.3	1241.4	-100.5	121.9	28.9	0.4	0.	-1.9	126.2
220.00	65.49	35.53	2044.4	1250.6	-111.7	84.5	25.5	1.2	0.	-13.1	126.2
221.00	65.77	35.53	2058.6	1259.7	-120.1	65.6	29.8	1.5	0.	-21.4	126.3
222.00	66.04	35.53	2072.8	1268.8	-127.7	62.0	31.2	1.4	0.	-28.9	126.3
223.00	66.30	35.53	2087.0	1277.9	-126.3	60.7	30.6	1.4	0.	-27.5	126.4
224.00	66.57	35.53	2101.2	1286.9	-124.8	60.2	30.2	1.4	0.	-25.9	126.4
225.00	66.82	35.52	2115.4	1296.0	-123.7	60.0	29.9	1.4	0.	-24.8	126.5
226.00	67.08	35.52	2129.7	1305.0	-122.8	59.9	29.6	1.4	0.	-23.9	126.6
227.00	67.33	35.52	2143.9	1314.0	-121.8	59.7	29.4	1.4	0.	-22.7	126.6
228.00	67.58	35.51	2158.2	1323.0	-120.5	59.4	29.2	1.4	0.	-21.3	126.7
229.00	67.83	35.50	2172.4	1332.0	-117.8	59.2	29.0	1.4	0.	-18.7	126.7
230.00	68.07	35.49	2186.7	1340.9	-116.7	59.1	28.7	1.4	0.	-17.5	126.8
231.00	68.31	35.49	2201.0	1349.9	-115.8	59.1	28.4	1.4	0.	-16.5	126.9
232.00	68.54	35.48	2215.3	1358.8	-115.2	59.4	28.1	1.4	0.	-15.8	126.9
233.00	68.78	35.46	2229.6	1367.7	-114.9	60.0	27.7	1.4	0.	-15.6	127.0
233.97	69.00	35.45	2243.4	1376.3	-114.7	60.2	27.5	1.4	0.	-15.3	127.0
235.00	69.23	35.44	2258.2	1385.4	-115.4	72.5	28.2	1.6	0.	-15.9	127.1
236.00	69.46	35.43	2272.5	1394.3	-104.2	99.0	26.7	1.1	0.	-4.7	127.1
237.00	69.68	35.42	2286.8	1403.1	-100.2	135.0	34.7	0.3	0.	-0.6	127.2
238.00	69.90	35.40	2301.1	1411.9	-99.6	152.5	52.3	0.1	0.	0.0	127.2
239.00	70.11	35.39	2315.4	1420.7	-97.0	156.6	66.1	0.3	0.	2.7	127.3

ACES TABULAR RESULTS

FIGURE 10

FIGURE 11

MISTRAM RATE STATION RECEIVED SIGNAL STRENGTH

TEST 4209 - 14 DECEMBER 1970

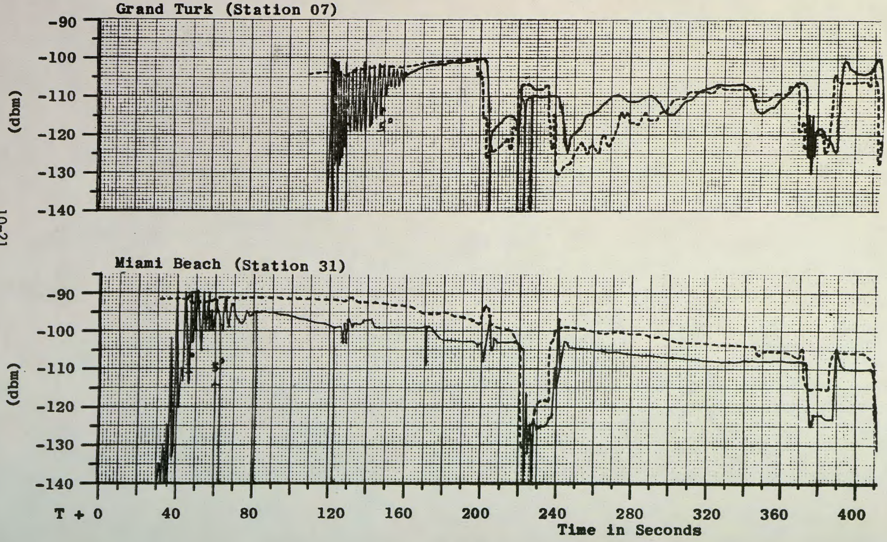

Grand Turk (Station 07)

Miami Beach (Station 31)